A virtual experiment for measuring system resilience: a case of chemical process systems
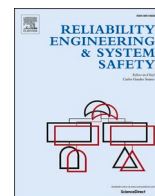
Sun, H.; Yang, M.; Wang, Haiqing

Important note
To cite this publication, please use the final published version (if applicable).
Please check the document version above.

A virtual experiment for measuring system resilience: A case of chemical process systems

Hao Sun [a,b], Ming Yang [b,c,*], Haiqing Wang [a,**]

[a] College of Mechanical and Electronic Engineering, China University of Petroleum (East China), Qingdao 266580, China
[b] Safety and Security Science Section, Department of Values, Technology, and Innovation, Faculty of Technology, Policy, and Management, Delft University of Technology, the Netherlands
[c] Centre of Hydrogen Energy, Institute of Future Energy, Universiti Teknologi Malaysia, UTM Johor Bahru, Johor 81310, Malaysia

ARTICLE INFO

ABSTRACT

Resilience is an emergent property of a system, which changes with various internal and external factors. Resilience is also a hidden property of a system that cannot be observed. Thus, experiments should be performed for a given system to measure its resilience. However, physical experiments are practically impossible. Inspired by the tensile test for the stress-strain curve in Material Science, this paper proposes a virtual experiment for measuring system resilience and applies it to a chemical process system. The physical parameters of system resilience of a process system are mapped to those of material resilience. A process system is viewed as a 'specimen' in this experiment. The system performance variation caused by disruptions is seen as the displacement of the specimen caused by the applied load. In absorption phase, the decrease speed of system performance is determined by the failure rate of components under disruptive condition. Response time, including fault diagnosis time and resource allocation time, is used to represent adaptation ability. Restoration ability depends on repair rate of components. For simplicity purpose, the proposed method is applied to resilience assessment of a release prevention barrier system used in the Chevron Richmond refinery crude unit and its associated upstream process.

1. Introduction

Chemical processes are essential for our society, but they also pose severe safety risks. Unfortunately, major process accidents continue to occur with the rapid growth of chemical process technologies. Process systems become more automated, digitalized, complex, and interdependent. This makes process systems vulnerable to uncertain disruptions (e.g., natural disasters, cyber-attacks, terrorism, etc.) [1]. Researchers have conducted enormous work to prevent and predict failures to ensure safety of process systems [2–9,32,35,37]. However, recurring accidents indicate that conducting traditional risk assessment alone to minimize risks at the design stage is insufficient to ensure system safety considering uncertain operating conditions and the socio-technological environment that a process system works in. People are well aware that no matter how robust our preventative or control methods are, we still have to handle the residue risk of highly uncertain events. This residue risk

also becomes evident from the continuous occurrence of severe process accidents [10,11]. Thus, there is a call to shift the focus of safety assessment from risk-oriented thinking to the paradigm of resilience engineering, which acknowledges the inherent uncertainty and complexity of system functioning and the need for performance variability [12–19,49,60].

The concept of resilience has drawn wide attention from academia as well as industries since it contributes to new ways of resisting disruptions and recovering adequately [20–27]. Resilience is a concept originally used in Material Science to describe the property of a material to spring back to its original state after undergoing deformation [28]. Later, the term resilience was gradually introduced into other scientific fields to measure the ability of a system to absorb changes and disturbances and maintain the original state [29–31]. Thus, various definitions of resilience have been proposed. The resilience of critical infrastructure is regarded as the ability to mitigate the degree of impact and/or duration of disruptions (NIAC, 2009). System resilience depends

Nomenclature

σ	stress
ε	strain
σ_a	the proportional limit
ε_a	strain corresponding to stress σ_a
σ_b	yield stress
ε_b	strain corresponding to stress σ_b
σ_c	the maximum stress that the material can withstand
ε_c	strain corresponding to stress σ_c
E	Young's modulus
P	applied load
A_0	the original specimen cross-sectional area
ΔL	displacement of the specimen caused by P
L_0	determines the original length of the specimen
σ_T	the engineering stress in TSSC
ε_T	the engineering strain in TSSC
σ_S	the average value of the impact of the disruption on each component in resilience engineering
ε_S	the degree of the system performance change caused by σ_S in resilience engineering
a'	disruption impact value in resilience engineering
a	the corresponding performance change caused by a'
b'	the maximum disruption intensity that the system can absorb in resilience engineering
b	the corresponding performance change caused by b'
c'	the maximum disruption intensity that the system can adapt to in resilience engineering
c	the corresponding performance change caused by c'
d'	the maximum disruption intensity that the system can recovery from in resilience engineering
d	the corresponding performance change caused by d'
I	disruption intensity
ΔS	performance change caused by disruption
N	the number of components of the system
S_0	the initial performance of the system
ε_{Si}	the performance change rate of the system caused by disruptions
F_T	the required for fault diagnosis
M_T	the start time of maintenance activities
RA_T	the required for resource allocation
R_e	recovery factor
D_S	diagnosis accuracy
RA_S	probability of successful resource allocation
M_S	the probability of successful maintenance

Acronyms

DBN	dynamic Bayesian network
SSC	stress strain curve
TSSC	true stress strain curve
RETSSC	resilience engineering true stress strain curve
CTPs	conditional probability tables
RPB	release prevention barrier

on its ability to anticipate, absorb, adapt to, and restore from disruptions. Fujita et al. [32] viewed resilience as the ability to resist and recover from accidents and natural events. Holling [33] defined the resilience of the ecosystem as the intrinsic property of the system, which is used to measure the persistence and ability of the ecosystem to absorb changes and disturbances and maintain the original species. Hosseini and Barker [34] considered resilience as the ratio of system performance recovery to system performance loss at a given disruption. Francis and Bekera [35] defined resilience as the comprehensive ability, comprising four attributes: absorption, adaptation, restoration, and learning.

Based on the aforementioned definitions, different resilience metrics and corresponding quantification approaches have been proposed. Wu et al. [36] developed an indicator-based method, which includes two indicators, i.e., traffic efficiency and safety performance, to assess the resilience of transportation networks during the post-earthquake long-term recovery period. Kammouh et al. [37] presented an indicator-based method, using three indicators, i.e., vulnerability, robustness, and recoverability, to quantify the resilience of engineering systems. Each indicator has its own sub-index. Dynamic Bayesian network is employed to represent the logic and structure relationship between resilience and these three indicators and various sub-indexes. After that, the system resilience can be determined. Sun et al. [15] developed another DBN model to assess the resilience of safety barriers for the process system. Chen et al. [38] presented an indicator-based method, which considers main characteristic factors (e.g., adaptability, resistance, and recovery), to assess urban resilience. Zinetullina et al. [39] presented a hybrid approach, which integrates the Functional Resonance Analysis Method (FRAM) and DBN to quantify system resilience. Belline et al. [40] proposed a Q-FRAM approach based on System Resilience Index (SRI) to assess the system's resilience. Yodo and Wang [41] developed a Bayesian network (BN)-based approach to quantifying reliability and restoration subject to disruptive events. Hosseini and Barker [34] introduced a novel method for quantifying resilience, including the ability of absorption, adaptation, and restoration, for inland waterway ports based on BN. Chen et al. [12] used storage capacity as the primary indicator of the hazardous material storage plants and introduced a dynamic stochastic approach to quantify the resilience. Cincotta et al. [42] proposed a method by considering vulnerability and recoverability to raise system resilience of firefighting strategies. Cai et al. [21] presented a DBN-based method to measure system resilience under different types of disruptions. Zhang et al. [26] developed a hybrid approach, which combines finite element models and DBN to quantify the resilience of mechanical structures. Yin et al. [43] proposed an approach, integrating knowledge-based method and data-driven method, to assess system resilience. Shandiz et al. [44] proposed a novel energy resilience framework, including three performance indicators, to plan and assess community energy resilience.

In the existing literature, resilience is often quantified based on mathematical models of system functional performance or performance index. In this paper, resilience is seen as a hidden, intrinsic, and emergent property of a system. As a concept originated from Material Science, we argue that system resilience can be measured via experiments similar to material resilience. Inspired by the tensile experiment for measuring material resilience in Materials Science, we aim to formulate an experiment to measure the resilience of chemical process systems. Since physical experiments for a complex system are practically impossible to perform at this stage, the present study proposes a virtual experiment for measuring the resilience of a chemical process system.

In existing resilience assessment metrics and models, the initial resilience is assumed as 1. Researchers believe resilience starts at 1 and then changes over time when disruption occurs, finally recovering to a new stable state. The purpose of those methods is assessing how resilience changes over time. As a contract, according to tensile experiment in Materials Science, the resilience of the specimen cannot be determined before the specimen is tested. Only when the experiment starts can the specimen's resilience be observed by performing the test. Thus, the system resilience measured by the virtual experiment in this manuscript starts from 0 rather than 1. As a result, the experiment-based method aims to measure the maximum resilience of system.

The proposed approach aims to measure resilience by a virtual

experimental approach. To develop a virtual experiment for this purpose, the physical parameters in the process system are compared with those in the material tensile experiment to form analogies. We aim to map the tensile experiment into the virtual experiment for measuring system resilience. The disruption intensity and system performance change are two critical parameters in the mapping process. The system performance in different process (i.e., absorption, adaptation, and restoration) can be determined by DBN. Firstly, duo to the impact of disruption, the failure rate of components will be increased, which make the system performance decrease rapidly. Secondly, adaptation ability is viewed as response capacity of system when disruption occurs, which can be represented by response time (*RT*). *RT* determines the time slice of DBN in the process of system performance degradation. Therefore, the process of system performance degradation depends on the ability of absorption and adaptation. After that, the restoration ability is dependent on repair rate of components. When maintenance measures are taken after *RT*, the system performance will increase. Therefore, the process of system performance increase depends on the ability of restoration. DBN is used to quantify the performance profile of system in the process of degradation and increase. The virtual experiment is developed to find their relationship, thus measuring system resilience. The contribution of the manuscript is providing a new way to define and quantify system resilience.

The remainder of this paper is organized as follows. Section 2 describes material resilience and how it can be measured and discusses the possibility of creating an experiment for measuring system resilience based on that for material resilience measurement. The proposed virtual experiment-based approach, including the DBN model and the resilience metric, is presented in Section 3. A case study is conducted in Section 4, followed by discussions in Section 5. Finally, Section 6 concludes this paper.

2. Material resilience versus system resilience

2.1. Stress-strain curve in Materials Science

The Stress-Strain curve (SSC), determined by tensile/compression experiments, is an essential concept in Materials Science, which is presented in Fig. 1.

In Fig. 1, the ordinate represents the stress, and the abscissa is the strain of the specimen. For SSC, in the early phase (stress below σ_a) of the curve, many materials follow Hooke's law (i.e., the stress is proportional to the strain), and the proportionality constant is the elastic
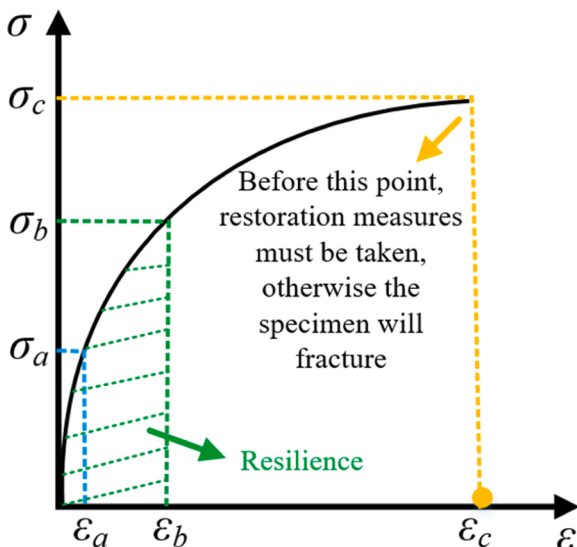
modulus or Young's modulus, expressed as *E* [46]. At this phase, the relationship between stress and strain is shown in Eq. (1). σ represents stress and ε is strain.

$$\sigma = E\varepsilon \tag{1}$$

In Fig. 1, the σ_a is the proportional limit, which means that when the stress is greater than σ_a, the stress and strain are no longer proportional. The σ_b indicates yield stress, which is an essential indicator of plastic materials. When the stress is less than σ_b, the specimen is able to restore to its original state after the stress is removed. In Material Science, the area under the SSC up to a given value of strain ε_b is termed the resilience of the specimen, which is shown in shaded area of the Fig. 1.

When the stress ranges from σ_b to σ_c, the strain increases significantly. If the stress is relieved at this time, the deformation of the specimen can only be partially recovered, while some residual deformation is retained. As the stress continues to increase, the material will eventually fracture.

2.2. The quantification of TSSC

The engineering stress σ_E and strain ε_E are determined by Eqs. (2) and (3) [45].

$$\sigma_E = \frac{P}{A_0} \tag{2}$$

$$\varepsilon_E = \frac{\Delta L}{L_0} \tag{3}$$

where *P* indicates applied load; A_0 is the original specimen cross-sectional area; ΔL represents the displacement of the specimen; L_0 determines the original length of the specimen.

A more efficient measure of the material's response in the plastic flow range can be obtained using the true stress σ_T instead of the engineering stress σ_E [45]. The true stress and strain can be described as Eqs. (4) and (5) [45]:

$$\sigma_T = \sigma_E(1 + \varepsilon_E) \tag{4}$$

$$\varepsilon_T = \ln(1 + \varepsilon_E) \tag{5}$$

According to Eqs. (3)-(5) can be converted into Eqs. (6) and (7). It can be seen from Eqs. (6) and (7) that there are only two variables: the applied load (*P*) and the displacement of the specimen (ΔL). Therefore, the main task of measuring material resilience is determining *P* and ΔL.

$$\sigma_T = \frac{P}{A_0}\left(1 + \frac{\Delta L}{L_0}\right) \tag{6}$$

$$\varepsilon_T = \ln\left(1 + \frac{\Delta L}{L_0}\right) \tag{7}$$

Based on Eqs. (6) and (7), the expression of σ_T with respect to ε_T can be expressed as Eq. (8). Based on Eq. (8), the true SSC (TSSC) can be determined.

$$\sigma_T = \frac{P \cdot e^{\varepsilon_T}}{A_0} \tag{8}$$

It is worth noting that, as for many materials, the relations mentioned above apply equally well if loads are placed to put the specimen in compression rather than tension.

2.3. The mapping process and virtual experiment

Once the relationship between stress and strain is determined, the function of TSSC can be obtained, i.e., Eq. (8). The area under the TSSC up to a given value of strain is termed the resilience of the specimen, which means that the resilience of the material can be determined by TSSC, which is shown in the shaded area of Fig. 1. To determine the

Fig. 1. The true stress-strain curve (adapted from Kweon et al. [45]).

TSSC, the applied load (P) and the displacement of the specimen (ΔL) should be measured.

When material ruptures in a tensile test, the experiment is terminated. Material restoration is not considered in TSSC. However, to measure system resilience in Resilience Engineering, restoration ability is an essential element that must be considered. Therefore, to take the restoration ability into account, we extend the TSSC to formulate a 'TSSC' for system resilience measurement in Resilience Engineering. It is named Resilience Engineering TSSC (RETSSC), shown in Fig. 2. The shaded area in Fig. 2 represents the extended area (i.e., restoration process), which is not considered in TSSC. The ordinate of Fig. 2 (i.e., ε_S) indicates the degree of the system performance change. The abscissa (i.e., σ_S) depends on the disruption intensity and performance loss, which can be seen in Eq. (9) in Table 1. The specific descriptions of critical points in Fig. 2 are presented in Table 1. It is worth noting that the increase speed from (c, c') to (d, d') is dependent on the maintenance resources, e.g., the number of maintenance teams. In other words, different maintenance resource will result in diffident rate of increase. Therefore, the curve may or may not be continuous at point (c, c').

In Resilience Engineering, a disruption affects the performance of process systems. This is similar to a load applied to a specimen that impacts the internal structure of specimens. As the disruption intensity increases, the performance of the process system may degrade. As long as the disruption is strong enough, the process system will malfunction eventually. Fig. 2 describes the process of performance change. It shows that when σ_S ranges from zero to b', the absorption ability of the system offsets the influence of disruption. The system returns to its original status. If σ_S ranges from b' to c', the impact of the disruption cannot be completed absorbed. This leads to a large performance change in the system. At this stage, the residual impacts can still be reduced by the adaptation ability of the system. When σ_S is larger than c', restoration measures must be implemented. Otherwise, the system remains in failure. The resilience of a process system can be measured based on RETSSC. A virtual experiment is then designed to generate RETSSC.

The physical parameters of system resilience are mapped from those of material resilience in Material Science. The mapping process is presented in Table 1. The intensity of disruptions I in Resilience Engineering is seen as the applied load P of Materials Science; The performance change of systems ΔS caused by disruptions can be viewed as the displacement (i.e., ΔL) resulting from the load P.

In the light of Eqs. (9) and (10) in Table 1, the expression of σ_S with respect to ε_S can be expressed as Eq. (11). It is worth noting that there are only two variables in Eqs. (9) and (10), namely I and ΔS. RETSSC developed based on these two variables is employed to measure the
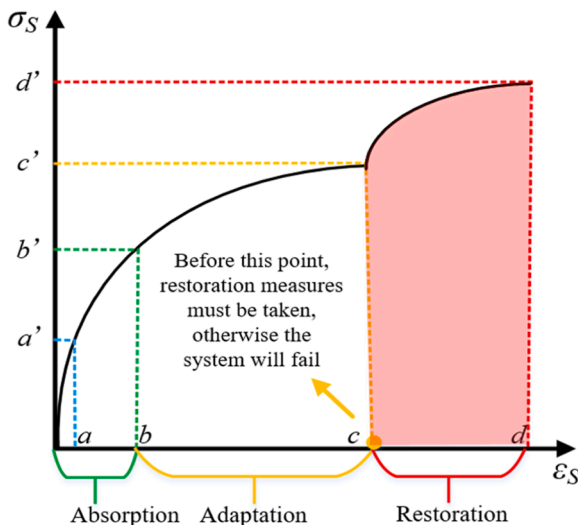

Fig. 2. The developed RETSSC based on TSSC.

Table 1

The analogy between TSSC in Materials Science and TSSC in Resilience Engineering

Key points of TSSC in Fig. 1 of Materials Science	Descriptions	Key points in RETSSC in Fig. 2 of Resilience Engineering	Descriptions
ε_T	Strain (the degree of deformation)	ε_S	The degree of the system performance change
σ_T	Stress (load value of per unit area)	σ_S	The average impact of a disruption on each component
Experiment variables	$P, \Delta L$	Virtual experiment variables	$I, \Delta S$
P	The load applied to the specimen	I	Intensity of disruptions
ΔL	Displacement of the specimen	ΔS	The amount of performance change
(ε_a, σ_a)	Proportionality limit	(a, a')	-
(ε_b, σ_b)	The yield stress, which is the maximum value of stress at which there is no permanent deformation	(b, b')	b' is the maximum disruption intensity that the system can absorb, which can be used to measure absorption ability
(ε_c, σ_c)	The fracture point.	(c, c')	c' is the maximum disruption intensity that the system can adapt to, which can be used to measure adaptation ability; In this point, restoration must be implemented. Otherwise, the system may fail.
		(d, d')	
-	-	(d, d')	d' is the maximum disruption intensity that the system can withstand after repair, which can be used to measure restoration ability
Key functions in TSSC of Materials Science	Number and description	Key functions in RETSSC of Resilience Engineering	Number and description
$\sigma_T = \dfrac{P}{A_0}\left(1 + \dfrac{\Delta L}{L_0}\right)$	Eq. (6)	$\sigma_S = \dfrac{I}{N}\left(1 + \dfrac{\Delta S}{S_0}\right)$	Eq. (9) where N is the number of components of the system; S_0 indicates the initial performance of the system.
$\varepsilon_T = \ln\left(1 + \dfrac{\Delta L}{L_0}\right)$	Eq. (7)	$\varepsilon_S = \ln\left(1 + \dfrac{\Delta S}{S_0}\right)$	Eq. (10)
$\sigma_T = \dfrac{P \cdot e^{\varepsilon_T}}{A_0}$	Eq. (8)	$\sigma_S = \dfrac{I \cdot e^{\varepsilon_S}}{N}$	Eq. (11)

system resilience. Therefore, the two main tasks of the proposed virtual experiment are to quantify I and ΔS.

$$\sigma_S = \frac{I \cdot e^{\varepsilon_S}}{N} \qquad (9)$$

The tensile/compression experiment aims to determine the relationship between applied load P and specimen displacement ΔL to measure the material resilience. The developed virtual experiment attempts to identify the relationship between disruption intensity I and system performance change ΔS to measure the system resilience. Like

the definition of resilience in Materials Science, the area under the RETSSC up to a given value of ε_S can be regarded as the resilience of process systems. Therefore, Eq. (11) can be converted to Eq. (12) to measure the resilience of process systems. Based on the aforementioned above, the system resilience R can be observed and measured with this virtual experiment.

$$R = \int_0^{\varepsilon_{Si}} \sigma_S d\varepsilon_S \tag{10}$$

where R indicates the system resilience, ε_{Si} represents the performance change rate of the system caused by disruptions.

According to the resilience quantification method of specimen in

Material Science, the area below the RETSSC at different stages is used to represent absorption, adaptation and restoration capacity, and then quantify system resilience in Resilience Engineering. Therefore, the system resilience R can be considered as the maximum amount of disruption impacts that the system can deal with without failing. The larger the R the better the resilience of the system.

3. The proposed methodology

The methodology is proposed to measure the system resilience. It comprises two main tasks: determining disruption intensity (I) and quantifying the performance change of the system (ΔS). A virtual experiment is developed to obtain RETSSC. Fig. 3 presents three main
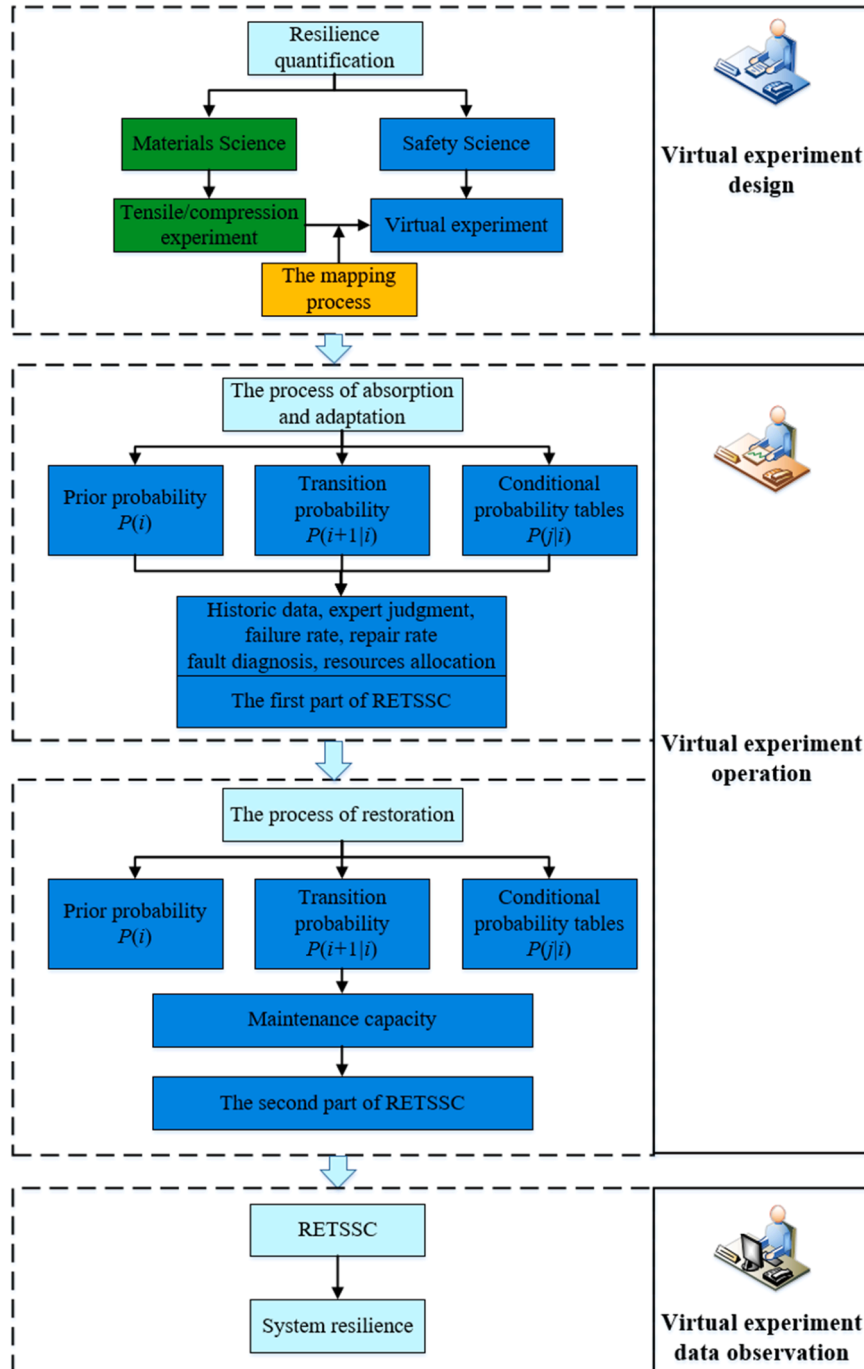
Fig. 3. The proposed methodology for assessing the system resilience.

parts of the virtual experiment: experiment design, experiment operation, and experiment data observation. The virtual experiment design has been discussed in Section 2.3. The rest of this section focuses on discussing the virtual experiment operation and experiment data observation.

In the phase of virtual experiment operation, the process of absorption, adaptation, and restoration is represented and measured by DBN. Firstly, a DBN model is developed to determine the system performance change in the process of absorbing and adapting to the disruption. *RT* is utilized to determine time slice in this process. The DBN is then adjusted according to repair rate of components to quantify the system performance change of the restoration process in different time-varying sequences. In accordance with the results of virtual experiment operation, a novel resilience metric is proposed to quantify the system resilience in the phase of experiment data observation. The details are presented in the following sections.

3.1. Quantification of the first part of RETSSC

At the stage of virtual experiment operation, the first task is to measure the system performance in the process of absorption and adaptation.

As an extension of BN in the time domain, in general, the structure and principles of DBN are the same as BN [47,48]. The exception is that DBN contains more than one time slice. The relationship among time slices can be described by transition probabilities. The structure of DBN is shown in Fig. 4.

In the normal degradation process, the prior probability of root factors and the conditional probability tables (CPTs) can be determined by the historical data and expert judgment [15,21,49,50]. Transition probabilities can be determined by failure rate λ and repair rate μ from OREDA and relevant literature. The probability is determined through a Markov-state transition relationship and is expressed as follows [51]:

$$p(X_{t+\Delta t} = work | X_t = work) = e^{-\lambda \Delta t} \tag{11}$$

$$p(X_{t+\Delta t} = fail | X_t = work) = 1 - e^{-\lambda \Delta t} \tag{12}$$

$$p(X_{t+\Delta t} = fail | X_t = fail) = e^{-\mu \Delta t} \tag{13}$$

$$p(X_{t+\Delta t} = work | X_t = fail) = 1 - e^{-\mu \Delta t} \tag{14}$$

The duration of external disruption (e.g., cyber-attacks, sabotage, etc.) is very short compared to the absorption, adaptation, and recovery time. As a result, the external disruption can be regarded as instantaneous [26]. When a disruption impacts the system, the failure rate of root nodes will increase, which is dependent on the disruption intensity (*I*). The larger the disruption intensity (*I*), the higher the failure rate of the root nodes. A high-intensity disruption may lead to the common cause failure of nodes [51]. The failure rate of the root nodes after disruption is determined by Eq. (17) [52].

$$\lambda_D = g_I \cdot \lambda_0 \tag{15}$$

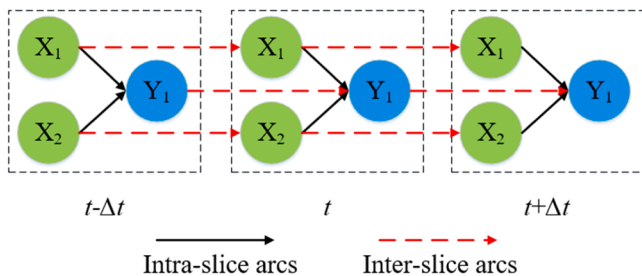where λ_D indicates failure rate of root nodes under disruption condition,

λ_0 represents initial failure rate of root nodes, g_I g denotes the score of dsiruption, which can be obtained from experimental data, historical data or expert opinion [53].

In the present study, DBN is used to determine the system performance under normal and disruptive conditions. The performance difference between them is defined as the performance change (i.e., $\triangle S$). Then $\triangle S$ is used in Eqs. (9) and (10), and Eq. (11) to obtain the first part of RETSSC. After this, the ability of absorption and adaptation can be determined. We assume that no external maintenance measures are taken in the process of absorbing and adapting to disruptions. The period between the occurrence of disruptions and the beginning of maintenance activities is defined as response time (*RT*), which can be determined by fault diagnosis time and resources allocation time [21]. In other words, system performance change during this period depends only on the ability of absorption and adaptation.

3.2. Quantification of the second part of RETSSC

The second task of virtual experiment operation is to measure the restoration process. The structure of the DBN model remains unchanged. However, when the maintenance measures are taken, the system performance will be enhanced. The repair rate of components is used to determine the transition probability of the DBN model to calculate the system performance in the process of restoration.

The maintenance measures start only after completing the related work of fault diagnosis and resource allocation. Fault diagnosis aims to identify the nodes that need to be repaired. Resource allocation is to rationally allocate and utilize existing resources to conduct maintenance activities under the condition of limited maintenance resources. Therefore, the sum of the time required for fault diagnosis (F_T) and resource allocation (RA_T) determines the response time(*RT*), which is expressed as Eq. (18). Furthermore, Eq. (18) can also be used to determine the number of time slices of the DBN developed for the process of absorption and adaptation.

$$RT = F_T + RA_T \tag{16}$$

Once the repair activities begin, the system performance will be increased. The transition probabilities in DBN are determined by repair rates. The difference between improved performance and initial performance (before maintenance measures are intervened) of a system can be regarded as $\triangle S$. $\triangle S$ is then applied to Eqs. (9) and (10), and Eq. (11) to obtain the second part of RETSSC. Hence, the restoration capacity can be determined. By combining the first and second parts of RETSSC, a complete RETSSC can be obtained. In the light of the complete RETSSC, system resilience can be measured based on Eq. (12).

4. Case study

On August 6, 2012, a leakage accident originated from a pipe rupture in a crude distillation unit in the Chevron Richmond refinery occurred, resulting in a fire accident eventually. Fortunately, no one was injured in the accident [11]. The fire accident resulted from the "4-side cut" leaving the Richmond refinery's C-1100 Crude unit atmospheric column [3], causing flammable light oil released at the rate of 10,800 barrels per day [11]. The specific information regarding the Richmond refinery accident can be found in the CSB investigation report [11]. The process of the Chevron Richmond refinery crude unit and its associated upstream process is shown in Fig. 5. To prevent the release accident, the release prevention barrier of the Chevron Richmond refinery crude unit is used to demonstrate the proposed methodology.

4.1. Quantification of the first part of RETSSC

The release prevention barrier of the Chevron Richmond refinery crude unit is used to demonstrate the proposed methodology. The first task is to determine the components in the release prevention barrier
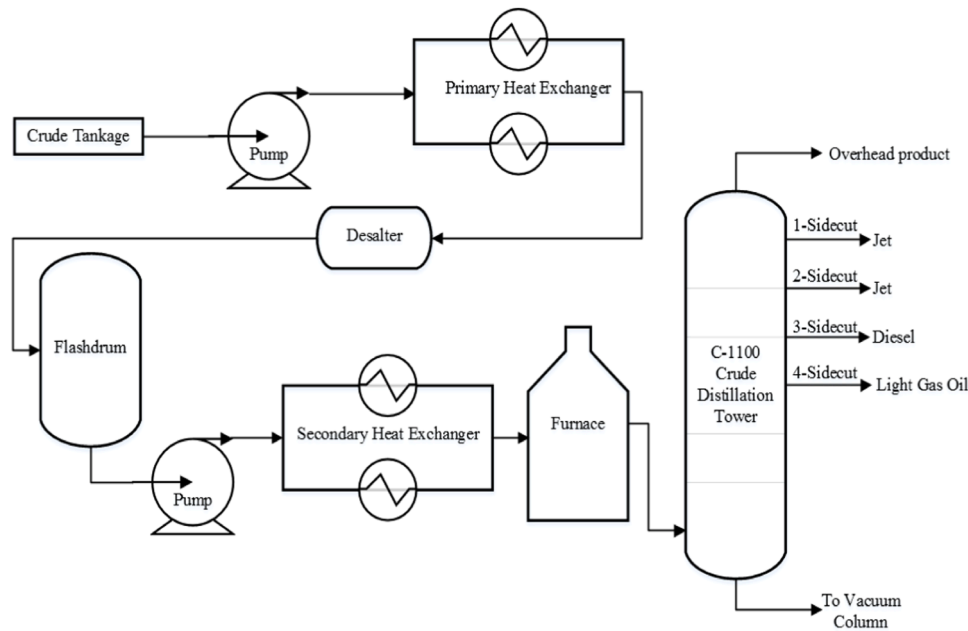

Fig. 4. The structure of DBN.

Fig. 5. Schematic diagram of the Chevron Richmond refinery crude unit.

(RPB) based on the process of the Chevron Richmond refinery and the accident report [11]. In this case, the RPB comprises four main secondary barriers:

- *Human factors barrier-* utilized to respond to an abnormal situation, which involves human actions and inactions.
- *Process control barrier-* attempts to use sensors/monitors, alarms, and controllers to keep the key parameters of the system within a safe range.
- *Facilities and equipment barrier-* employs the physical and technical barrier to prevent the leakage and escalation events.
- *Management and organizational barrier-* in the effort to use reasonable rules and regulations to ensure the safe behavior of workers and the safe state of equipment.

The specific components of RPB and the corresponding DBN model are shown in Table 2 and Fig. 6.

Safety barrier is a typical critical safety equipment (SCE). Its performance is often indicated by "availability", a dimensionless value defined in reliability engineering. The developed DBN model is employed to quantify the performance change of the release prevention barrier (RPB). Firstly, the system performance under the normal condition (i.e., before the disruption) should be identified by the DBN. The initial data of the DBN model are identified by historical data and expert judgment. Moreover, when a disruption occurs at the system, the failure rates of the basic components are increased, and the failure rates of basic components can be determined by Eq. (17) and Table 2. The disruption intensity (I) is assumed as 0.8 to illustrate the proposed methodology. Through considering the actual situation of historical data, the process of the fault diagnosis needs 2 hours; the process of the resource allocation requires 6 h. According to Eq. (18), RT is 8 h. Therefore, the number of time slices for the DBN in the process of absorption and adaptation is 8 h. In other words, maintenance measures are taken at 8 h after disruption occurs.

In accordance with the failure data of each component and the developed DBN model, the performance functions of the system under the normal and disruption condition can be determined. According to the aforementioned above, the performance curve and the performance change curve of the RPB in the process of absorption and adaptation are presented in Fig. 7.

Table 2
The specific information of components for the RPB system.

Symbol	Description	Initial Prior probability	Initial failure rateλ	Initial Repair rate
X_1	Supervision	0.001	-	-
X_2	Skill	0.001	-	-
X_3	Experience	0.001	-	-
X_4	Knowledge	0.001	-	-
X_5	Work permit	0.007	-	-
X_6	Work procedure	0.005	-	-
X_7	Flow controller	0.00178	5.72×10^{-5}	0.02
X_8	Temperature controller	0.00198	5.72×10^{-5}	0.02
X_9	Temperature monitor	0.00146	4.66×10^{-5}	0.023
X_{10}	Temperature alarm	0.00158	6.54×10^{-5}	0.022
X_{11}	Pressure monitor	0.00242	4.66×10^{-5}	0.023
X_{12}	Pressure alarm	0.00167	6.54×10^{-5}	0.022
X_{13}	Pump	0.0005	4.05×10^{-5}	0.014
X_{14}	Valve	0.0003	6.13×10^{-5}	0.021
X_{15}	Flange	0.00032	-	-
X_{16}	Protective coating	0.00062	-	-
X_{17}	Cathodic protection	0.00053	-	-
X_{18}	Maintenance procedure	0.005	-	-
X_{19}	Repair procedure	0.005	-	-
X_{20}	Testing	0.003	-	-
X_{21}	Routing inspection	0.050	-	-
X_{22}	Education	0.0004	-	-
X_{23}	Training	0.0004	-	-
X_{24}	Safety culture	0.005	-	-

Under normal condition, due to the degradation of components, the system performance decreases from 1 to 0.905. Therefore, the initial system performance is defined as 0.905. When the disruption occurs, the components of the system will be affected, leading to the performance decreases. Due to the required time for finishing fault diagnosis and resource allocation is 8 hours, thus, the system performance drops from 0.905 to 0.206 after 8 h. The performance curve can be determined by the developed DBN, as shown in Fig. 7 (i.e., the black curve). The performance change curve of the system can be determined by the system's
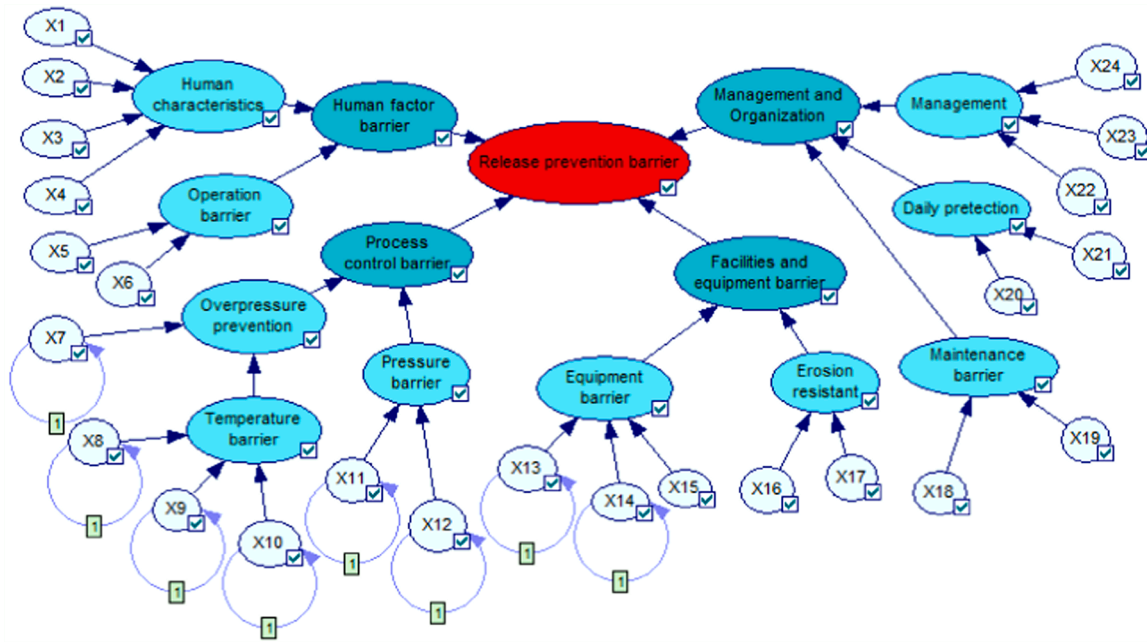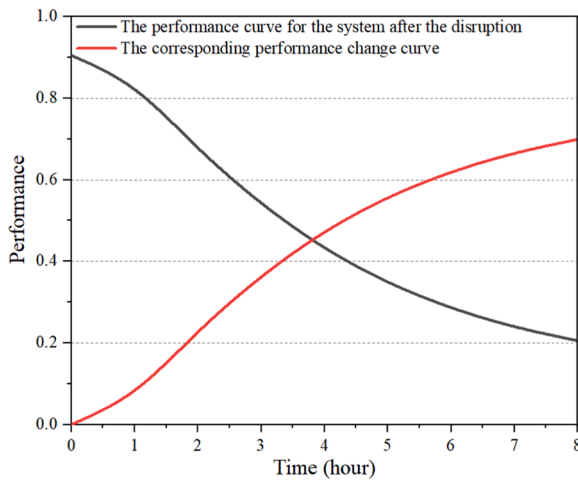
Fig. 6. The DBN model for the RPB.

Fig. 7. The performance curve and the performance change curve for the RPB in the process of absorption and adaptation.
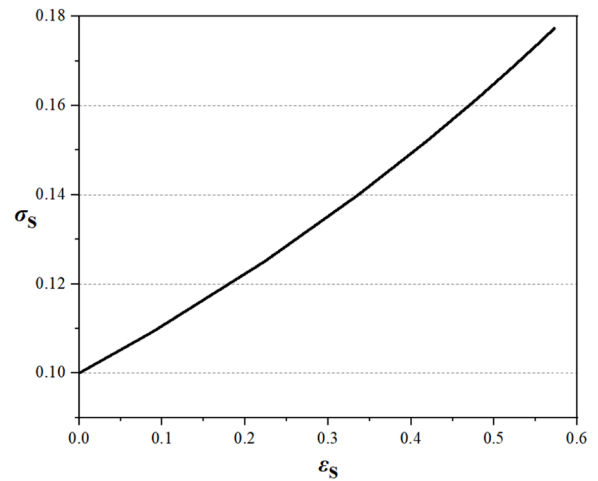

Fig. 8. The first part of RETSSC in the process of absorption and adaptation for RPB.

initial state and performance curve, which is depicted as the red curve of Fig. 7. In accordance with Fig. 7, Eq. (9), Eq. (10), and Eq. (11), the first part of RETSSC Resilience Engineeringcan be determined, which is sketched in Fig. 8. It can be seen from Fig. 8, when the σ_S increases from 0.1 to 0.177, the ε_S increases from 0 to 0.573. The process of the performance change in Fig. 8 is dependent on the ability of absorption and adaptation of the system.

It can be seen from Fig. 9, for the same ε_S, the greater the σ_S, the greater of the system resilience. In other words, under the condition of the same performance variation, the stronger the disruption intensity the system can withstand, the better the resilience of the system. Therefore, improving the ability of absorption and adaptation can enhance the system's ability to handle the effects of disruption, thus reinforcing the system resilience.

4.2. Quantification of the second part of RETSSC

As the aforementioned in Section 2.3, the TSSC of Materials Science

does not include restoration ability. Thus, Fig. 2 is developed to extend the TSSC to consider the restoration ability of the system resilience. With maintenance activities, the system performance is enhanced. According to Table 2, the transition probabilities can be determined by repair rate. As a result, the system performance curve and performance change curve are shown in Fig. 10. It can be seen from Fig. 10, duo to the maintenance measures, the system performance is enhanced from 0.206 to 0.905, which takes system 24 hours to recovery from the impact of disruption. After that, the system performance reaches an equilibrium state. The specific information of system performance change is depicted in Fig. 10.

In the light of Fig. 10, Eqs. (9) and (10), and Eq. (11), the second part of RETSSC can be determined, which is shown in Fig. 11. From Fig. 11, we can see that when the σ_S increases from 0.177 to 0.249, the ε_S increases from 0.573 to 0.912. The process of the curve change in Fig. 11 depends on the restoration ability of the system.

It is worth noting that, there is no maintenance measures for specimen in tensile experiment of Material Science. Therefore, the
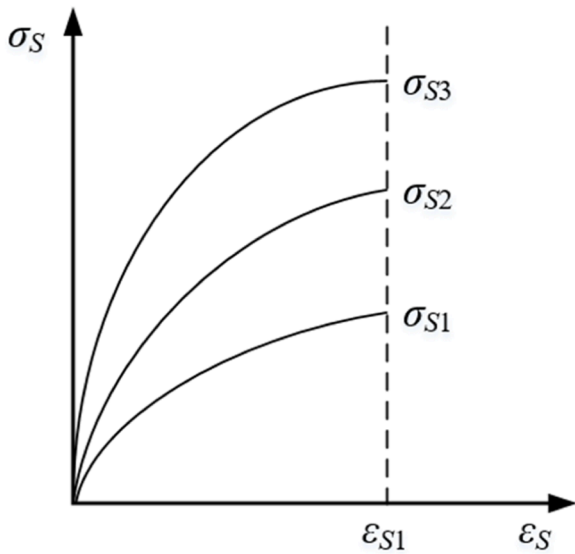
Fig. 9. The different first part of RETSSC caused by different absorption and adaptation ability.
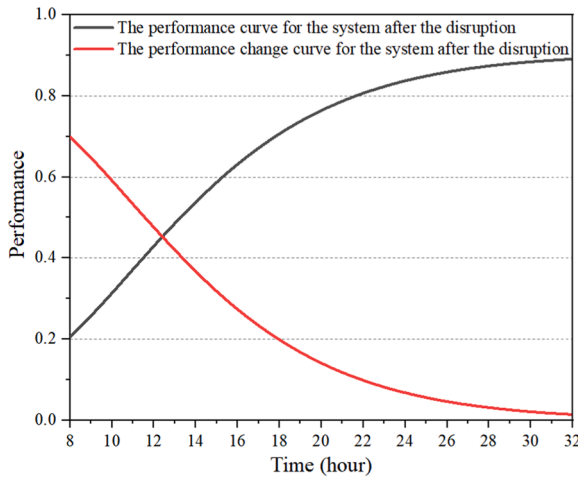
Fig. 10. The performance curve and the performance change curve for the RPB in the process of restoring from the disruption.
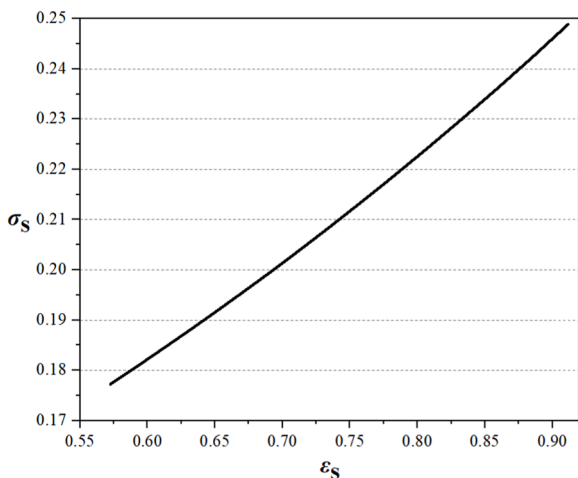
Fig. 11. The second part of RETSSC for RPB.

restoration ability is not considered in TSSC. As a contrast, for a process system, the maintenance measures can be used to increase system performance after disruption. Therefore, by comparing Figs. 8 and 11 it can be concluded that duo to the restoration ability, the ability of system to deal with disruption is larger than that of a system without restoration ability.

4.3. Quantification of the system resilience

Based on Fig. 8 (the first part of RETSSC) and Fig. 11 (the second part of RETSSC), the complete RETSSC can be determined and shown in Fig. 12. The black line in Fig. 12 indicates the first part of the RETSSC considering the process of absorption and adaptation, and the blue line stands for the second part of the RETSSC, including the restoration process. In other words, due to the intervention of maintenance activities, the system can withstand greater disruption intensity than that of the system without restoration ability. The combination of the two parts formulates the complete RETSSC. According to Fig. 12 and Eq. (12), the system resilience of the RPB can be measured, as shown in Fig. 13.

It can be seen from Fig. 13 that the resilience of the system starts from 0. This is because the resilience in this present study is measured by the proposed virtual experiment, which can be regarded as the 'observed resilience'. When the virtual experiment starts, the system resilience is able to be observed and measured. This is like the resilience of specimens in tensile experiment in Materials Science: the resilience of the specimen cannot be determined before the specimen is tested. Only when the experiment starts can the specimen's resilience be observed step by step.

In the beginning, due to the relevant work (i.e., fault diagnosis and resource allocation) requiring time to complete, no maintenance activities could be conducted during this period. In this process, the absorption ability mitigates the influence of the disruption on the system. On this basis, adaptation ability determines the response time (*RT*). Due to the positive effect of these two types of ability, the system resilience increases gradually at the first stage (i.e., the black line in Fig. 13). After this, maintenance measures will be taken at 8 hours when fault diagnosis and resource allocation are completed. Owing to the intervention of maintenance activities, the system resilience increases from 0.077 to 0.149. In other words, if the restoration ability is not considered in the system (e.g., a specimen), the system resilience is 0.077. For RPB, duo to the impact of restoration ability, the system resilience is enhanced from 0.077 to 0.149. Therefore, the restoration ability is a critical element of system resilience.
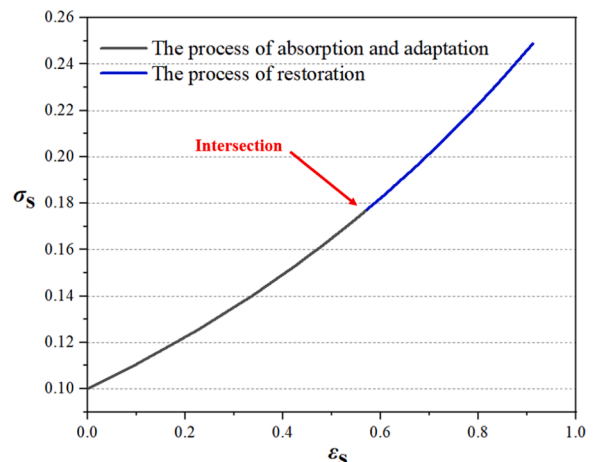
Fig. 12. The complete RETSSC of Resilience EngineeringRPB.

Yang: Conceptualization, Methodology, Formal analysis, Writing – review & editing, Validation. Haiqing Wang: Supervision, Writing – review & editing, Funding acquisition.

Declaration of Competing Interest

The research being report in this paper titled "**A virtual experiment for measuring system resilience: a case of chemical process systems**" was supported by China University of Petroleum and Delft University of Technology. The authors of this paper have the IP ownership related to the research being reported. The terms of this arrangement have been reviewed and approved by the university in accordance with its policy on objectivity in research.

Data availability

Data will be made available on request.

References

[1] Sun H, Wang H, Yang M, Reniers G. Towards limiting potential domino effects from single flammable substance release in chemical complexes by risk-based shut down of critical nearby process units. Process Saf Environ Prot 2021;148:1292–303.

[2] Abbassi R, Khan F, Garaniya V, Chai S, Chin C, Hossain K. An integrated method for human error probability assessment during the maintenance of offshore facilities. Process Saf Environ Prot 2015;94:172–9.

[3] Adedigba SA, Khan K, Yang M. An integrated approach for dynamic economic risk assessment of process systems. Process Saf Environ Prot 2018;116:312–23.

[4] Fakhravar D, Khakzad N, Reniers G, Cozzani V. Security vulnerability assessment of gas pipelines using Discrete-time Bayesian network. Process Saf Environ Prot 2017;111:714–25.

[5] George PG, Renjith VR. Evolution of safety and security risk assessment methodologies towards the use of bayesian networks in process industries. Process Saf Environ Prot 2021;149:758–75.

[6] Ji ZZ, Yang SH, Cao Y, et al. Harmonizing safety and security risk analysis and prevention in cyber-physical systems. Process Saf Environ Prot 2021;148:1279–91.

[7] Khakzad N. System safety assessment under epistemic uncertainty: using imprecise probabilities in Bayesian network. Saf Sci 2019;116:149–60.

[8] Landucci G, Argenti F, Cozzani V, Reniers G. Assessment of attack likelihood to support security risk assessment studies for chemical facilities. Process Saf Environ Prot 2017;110:102–14.

[9] Misuri A, Cozzani V. A paradigm shift in the assessment of Natech scenarios in chemical and process facilities. Process Saf Environ Prot 2021;152:338–51.

[10] CSB, 2007. BP America Refinery Explosion Texas City, TX, March 23, 2005, Final Report finding, http://www.csb.gov/, (last checked 16.10.14).

[11] CSB, 2014. Chevron richmond refinery pipe rupture and fire California, CA, August 6, 2012 final report finding, http://www.csb.gov/, (last checked 17.11.14).

[12] Chen C, Yang M, Reniers G. A dynamic stochastic methodology for quantifying HAZMAT storage resilience. Reliab Eng Syst Saf 2021;215:107909.

[13] Jain P, Pasman H, Mannan MS. Process system resilience: from risk management to business continuity and sustainability. Int J Bus Continuit Risk Manag 2020;10:47–66.

[14] Pasman H, Kottawar K, Jian P. Resilience of process plant: what, why, and how resilience can improve safety and sustainability. Sustainability 2020;12:6152.

[15] Sun H, Wang H, Yang M, Reniers G. Resilience-based approach to safety barrier performance assessment in process systems. J Loss Prev Process Ind 2021;73:104599.

[16] Abimbola M, Khan F. Resilience modeling of engineering systems using dynamic object-oriented Bayesian network approach. Comput Ind Eng 2019;130:108–18.

[17] Jain P, Rogers WJ, Pasman H, Keim KK, Mannan MS. A Resilience-based Integrated Process Systems Hazard Analysis (RIPSHA) approach: Part I plant system layer. Process Saf Environ Prot 2018;148:92–105.

[18] Xiao YH, Zhao XD, Wu YP, et al. Seismic resilience assessment of urban interdependent lifeline networks. Reliab Eng Syst Saf 2022;218:108164.

[19] Zhou J, Coit DW, Felder FA, Wang DL. Resiliency-based restoration optimization for dependent network systems against cascading failures. Reliab Eng Syst Saf 2021;207:107383.

[20] Abaei MM, Hekkenberg R, Toroody AB, et al. A probabilistic model to evaluate the resilience of unattended machinery plants in autonomous ships. Reliab Eng Syst Saf 2021;219:108176.

[21] Cai BP, Zhang YP, Wang HF, et al. Resilience evaluation methodology of engineering systems with dynamic-Bayesian-network-based degradation and maintenance. Reliab Eng Syst Saf 2021;209:107464.

[22] Cassottana B, Shen L, Tang LC. Modeling the recovery process: a key dimension of resilience. Reliab Eng Syst Saf 2019;190:106528.

[23] Fan DM, Sun B, Dui HY, et al. A modified connectivity link addition strategy to improve the resilience of multiplex networks against attacks. Reliab Eng Syst Saf 2022:108294.

[24] Tabandeh A, Sharma N, Gardoni P. Uncertainty propagation in risk and resilience analysis of hierarchical systems. Reliab Eng Syst Saf 2022;219:108208.

[25] Zhang C, Xu X, Dui HY. Resilience measure of network system by node and edge indicators. Reliab Eng Syst Saf 2020;202:107035.

[26] Zhang YP, Cai BP, Liu YL, Jiang QQ, Li WC, Feng Q, Liu YH, Liu GJ. Resilience assessment approach of mechanical structure combining finite element models and dynamic Bayesian networks. Reliab Eng Syst Saf 2021;216:108043.

[27] Zhang ZY, Ji TT, Wei HH, et al. Dynamic emergency inspection routing and restoration scheduling to enhance the post-earthquake resilience of a highway–bridge network. Reliab Eng Syst Saf 2022;220:108282.

[28] Darling KA, Kale C, Turnage S, et al. Nanocrystalline material with anomalous modulus of resilience and springback effect. Scripta Materialia 2017;141:36–40.

[29] Jamaluddin K, Alwi S, Manan Z, Hamzah K, Klemes J. Hybrid power systems design considering safety and resilience. Process Saf Environ Prot 2018;120:256–67.

[30] Pramoth R, Sudha S, Kalaiselvam S. Resilience-based Integrated Process System Hazard Analysis (RIPSHA) approach: application to a chemical storage area in an edible oil refinery. Process Saf Environ Protect 2020;141:246–58.

[31] Todman LC, Fraser FC, Corstanje R, et al. Defining and quantifying the resilience of responses to disturbance: a conceptual and modelling approach from soil science. Sci Rep 2016;6:28426.

[32] Fujita H, Gaeta A, Loia V, Orciuoli F. Resilience analysis of critical infrastructures: a cognitive approach based on granular computing. IEEE Trans Cybern 2019;49:1835–48.

[33] Holling CS. Simplifying the complex: the paradigms of ecological function and structure. Eur J Oper Res 1987;30:139–46.

[34] Hosseini S, Barker K. Modeling infrastructure resilience using Bayesian networks: a case study of inland waterway ports. Comput Ind Eng 2016;93:252–66.

[35] Francis R, Bekera B. A metric and frameworks for resilience analysis of engineered and infrastructure systems. Reliab Eng Syst Saf 2014;121:90–103.

[36] Wu YY, Hou GY, Chen SR. Post-earthquake resilience assessment and long-term restoration prioritization of transportation network. Reliab Eng Syst Saf 2021;211:107612.

[37] Kammouh O, Gardoni P, Cimellaro GP. Probabilistic framework to evaluate the resilience of engineering systems using Bayesian and dynamic Bayesian networks. Reliab Eng Syst Saf 2020;198:106813.

[38] Chen CK, Xu LL, Zhao DY, Xu T, Lei P. A new model for describing the urban resilience considering adaptability, resistance and recovery. Saf Sci 2020;128:104756.

[39] Zinetullina A, Yang M, Khakzad N, Golman B, Li XH. Quantitative resilience assessment of chemical process systems using functional resonance analysis method and dynamic Bayesian network. Reliab Eng Syst Saf 2021;205:107232.

[40] Belline E, Coconea L, Nesi P. A functional resonance analysis method driven resilience quantification for socio-technical systems. IEEE Syst J 2020;14:1234–44.

[41] Yodo N, Wang P. Resilience modeling and quantification for engineered systems using Bayesian networks. J Mech Des 2016;138:031404.

[42] Cincotta S, Kahkzad N, Cozzani V, Reniers G. Resilience-based optimal firefighting to prevent domino effects in process plants. J Loss Prev Process Ind 2019;58:82–9.

[43] Yin JT, Ren XL, Liu RH, Tang T, Su S. Quantitative analysis for resilience-based urban rail systems: a hybrid knowledge-based and data-driven approach. Reliab Eng Syst Saf 2022;219:108183.

[44] Shandiz SC, Foliente G, Rismanchi B, et al. Resilience framework and metrics for energy master planning of communities. Energy 2020;203:117856.

[45] Kweon HD, Kim JW, Song O, Oh D. Determination of true stress-strain curve of type 304 and 316 stainless steels using a typical tensile test and finite element analysis. Nucl Eng Technol 2021;53:647–56.

[46] Dovstam K. Augmented Hooke's law in frequency domain. A three dimensional, material damping formulation. Int J Solids Struct 1995;32:2835–52.

[47] Huang KX, Chen GH, Khan F, Yang YF. Dynamic analysis for fire-induced domino effects in chemical process industries. Process Saf Environ Prot 2021;148:686–97.

[48] Khan F, Rathnayaka S, Ahmed S. Methods and models in process safety and risk management: past, present and future Process. Saf Environ Prot 2015;98:116–47.

[49] CCPS. Guidelines for process equipment reliability data with data tables. New York, USA: Center for Chemical Process Safety; 1989.

[50] Zarei E, Azadeh A, Khakzad N, Aliabadi MM, Mohammadfam I. Dynamic safety assessment of natural gas stations using Bayesian network. J Hazard Mater 2017;321:830–40.

[51] Cai BP, Xie M, Liu YH, Liu YL, Feng Q. Availability- based engineering resilience metric and its corresponding evaluation methodology. Reliab Eng Syst Saf 2018;172:216–24.

[52] Xie L, Habrekke S, Liu YL, et al. Operational data-driven prediction for failure rates of equipment in safety instrumented systems: a case study from the oil and gas industry. J Loss Prev Process Ind 2019;60:96–105.

[53] Brissaud F, Charpentier D, Fouladirad M, et al. Failure rate evaluation with influencing factors. J Loss Pre Process Ind 2010;23:187–93.